Transport properties in a spin polarized gas, III

C. Lhuillier

Tome 44 N° 1 JANVIER 1983

LE JOURNAL DE PHYSIQUE

J. Physique **44** (1983) 1-12 JANVIER **1983**, PAGE 1

Classification
Physics Abstracts
51.10 — 67.20

Transport properties in a spin polarized gas, III

C. Lhuillier

Laboratoire de Spectroscopie Hertzienne de l'Ecole Normale Supérieure,
24, rue Lhomond, 75231 Paris Cedex 05, France

(*Reçu le 11 juin 1982, accepté le 27 septembre 1982*)

Résumé. — Les coefficients de transport des gaz quantiques polarisés (^{3}He, H↑ et D↑) ont été calculés dans le domaine de température 0,04-10 K pour une polarisation nucléaire **M** quelconque ($0 \leqslant M \leqslant 1$). Après une analyse en ondes partielles des caractéristiques des collisions dans les trois systèmes, on étudie les différentes « sections efficaces » directes et d'échange qui sont nécessaires pour décrire la collision de deux atomes polarisés. Les conséquences de l'indiscernabilité des particules se manifestent macroscopiquement par de nombreux effets : parmi ceux-ci on étudie ici la variation de la conduction de la chaleur en fonction de la polarisation nucléaire du milieu, l'existence d'un couplage entre les modes de diffusion de la chaleur et de la composante longitudinale du spin et le caractère oscillatoire de l'évolution des composantes transverses du spin.

Abstract. — A complete quantum phase shift calculation of several transport coefficients in spin polarized quantum gases (^{3}He, H↑ and D↑) has been carried out for temperatures ranging from 0.04 K to 10 K and nuclear polarizations M varying from 0 to 1. After a detailed analysis of the dynamical features of the collision, the various direct and exchange « cross sections » necessary to describe the collision between two spin-polarized atoms are studied. Emphasis is then placed on some particle-indistinguishability consequences that could be seen in ^{3}He or H↑ systems, such as the strong M dependence of the heat capacity, a mode coupling between heat capacity and longitudinal spin diffusion and the oscillatory character of the evolution of the transverse components of M.

Transport properties in spin-polarized gases were studied in two previous articles [1, 2] (hereafter called LL1 and LL2). At low temperatures, particle-indistinguishability effects may become essential during collisions and consequently strongly affect the non-equilibrium properties of macroscopic systems ([1]). Insofar as the nuclear polarization of the atoms can reinforce their indistinguishability, one can predict that transport properties not only in dense degenerate systems, but also in dilute, non-degenerate gases should be sensitive to nuclear polarization.

As was shown in LL1, due to symmetry effects, the collision between two spin-polarized atoms will generally affect both the kinetic and the nuclear variables of the impinging atoms. As a result the Boltzmann equation for the spin density operator exhibits, through its collision term, a strong dependence on the nuclear polarization described in the most general case by four independent « cross sections » : σ_k, σ_k^{ex}, τ_k^{ex}, τ_{fwd}^{ex} (equations (16) and (32) of LL1); σ_k is the standard differential cross section for distinguishable particles, σ_k^{ex}, τ_k^{ex}, τ_{fwd}^{ex} are three real independent functions of the scattering amplitude $f(\theta)$ which arise through exchange effects. To characterize these various terms further, it can be noticed that σ_k and σ_k^{ex} mainly govern the evolution of scalar and longitudinal variables (relative to the local spin direction). In the simple case where the directions of the spins are parallel everywhere in the sample, the medium can be described as a mixture of $(2I + 1)$ species (for the spin $I = 1/2$ case, the « up » and « down » species), the cross section for collisions of atoms in different spin states is simply σ_k (distinguishable « cross section ») and that for atoms in the same spin state is the properly symmetrized cross section $\sigma_k + \varepsilon\sigma_k^{ex}$ with $\varepsilon = +1$ (respectively -1) for bosons (respectively fermions). On the other hand τ_k^{ex} and τ_{fwd}^{ex} govern the evolution of transverse nuclear variables, they are associated with oscillatory and non-dissipative effects that we called in LL1 the « identical spin rotation » effects.

([1]) All the effects discussed here, as in LL1 and LL2, are due purely to the strong correlations induced by the Pauli principle between nuclear and translational variables and not to magnetic coupling between internal and external variables. These effects are therefore different from those discussed in molecular gases transport theory [3, 4].

On the macroscopic scale, this complexity of the collision term of the Boltzmann equation reveals itself in a wide variety of polarization-dependent effects. One can distinguish between the pure damping phenomena governed only by the two cross sections σ_k and σ_k^{ex}, and the phenomena with an oscillatory character that involve the two extra cross sections τ_k^{ex} and τ_{fwd}^{ex}. Among the first kind, there is the strong dependence of heat conduction and viscosity on nuclear polarization (equations (60) and (75) of LL1), and the existence of mode coupling between spin diffusion, heat conduction and eventually concentration diffusion in isotopic mixtures (equations (30) and (41) of LL2). Belonging to the second kind, there is the oscillatory behaviour of the transverse spin current which can result in spin waves in dilute media. Similar phenomena do exist in dense degenerate systems : the nuclear polarization dependence of heat conduction and viscosity has been studied by Bashkin and Meierovitch [5] in ^{3}He-^{4}He mixtures and the first experimental evidence has been very recently obtained by Greywall and Paalanen [6]. An oscillatory behaviour of the transverse spin current in dense ^{3}He was also predicted some years ago by Leggett [7] and observed experimentally by Corrucini and coworkers [8]. All this experimental evidence for indistinguishability is concerned with dense, degenerate, fermionic systems at very low temperatures. As a result of the work reported in LL1 and LL2 we can predict that such effects could manifest themselves both in bosonic and fermionic non-degenerate systems as soon as the temperature is low enough for the De Broglie wavelength to be comparable to the potential interaction range, whatever the density of the gas; for ^{3}He, H↑ and D↑ these effects must be significant as soon as the temperature is in the range of one kelvin. Moreover, in dilute systems the quantum mechanical analysis of binary collisions allows an *ab initio* calculation of all the predicted effects. With regard to recent experimental developments it appears that strong nuclear polarization can be achieved in H↑ [9] as well as in ^{3}He; it therefore seemed useful to give numerical estimates of the predicted effects. This was done with standard techniques : phase shift analysis of the collision, and numerical computation of the phase shifts [10] and collision integrals [11, 12] for the three systems H↑, D↑ and ^{3}He.

The aim of section 1 is to describe the main features of the collision in the three systems. None of these potentials is strong enough to accommodate bound states, but the phase shift analysis reveals some marked differences. In H↑ the effective interaction is essentially repulsive and weak whereas in D↑ or in ^{3}He the proximity of a virtual state leads to a larger, attractive, effective interaction in the low-energy limit. Differential and angular-averaged cross sections are then studied in the light of this analysis of the collision. In section 2 we report the results of our computation of the heat conduction coefficient, mode coupling between heat and spin diffusion and oscillatory transverse spin diffusion due to identical spin rotation effects.

1. **The collision in the quantum gases H↑, D↑, ^{3}He.** — 1.1 INTERACTION POTENTIALS. — In this study we have focussed our interest on the three lightest quantum systems : H↑, D↑, and ^{3}He. H↑ and D↑ are the electronic spin-polarized isotopes of hydrogen. Throughout this paper we suppose the electronic polarization to be complete and the hyperfine interaction negligible; in these limits H↑ and D↑ behave dynamically as a boson [13, 14] and a fermion respectively, whose nuclear spin $I = 1/2$ (or $I = 1$) is not coupled to external variables. The atoms only interact through the $^3\Sigma_u$ molecular potential. The best description of this potential for an internuclear distance r in the range of interest is that of Kolos and Wolniewicz [15]; we have used Silvera's fit [16]

$$V(r) = \exp(0.096\,78 - 1.101\,73\,r - 0.039\,45\,r^2) - \\ - \{\eta(r - 10.037\,8) + \eta(10.037\,8 - r) \\ \times \exp[-(10.037\,8/r - 1)^2]\} \\ \times (6.5/r^6 + 124/r^8 + 3\,285/r^{10}) \quad (1)$$

where all quantities are in atomic units and $\eta(x)$ is the unit step function defined by $\eta(x) = 0(1)$ if $x < 0(> 0)$.

For the ^{3}He system, where the interaction potential is not so well known, we have computed all quantities of interest for two pair potentials :

the widely used Lennard-Jones potential

$$V(r) = 4\,\varepsilon \times \left[\left(\frac{\sigma}{r}\right)^{12} - \left(\frac{\sigma}{r}\right)^{6}\right] \quad (2)$$

with $\varepsilon = 10.22$ K and $\sigma = 2.556$ Å,

and the HFDHE2 potential of Aziz *et al.* [17] which gives presently the best overall agreement with experiment :

$$V(r) = \varepsilon\left\{A \exp - \left(\frac{\alpha r}{r_m}\right) - \right. \\ - \left[C_6\left(\frac{r_m}{r}\right)^6 + C_8\left(\frac{r_m}{r}\right)^8 + C_{10}\left(\frac{r_m}{r}\right)^{10}\right] \\ \times \left[\eta(r - r_m) + \eta(r_m - r)\right. \\ \left.\left. \times \exp\left[-\left(\frac{Dr_m}{r} - 1\right)^2\right]\right]\right\} \quad (3)$$

with the following parameters values :

$A = 0.544\,850\,4 \times 10^6$	$\varepsilon = 10.8$ K
$\alpha = 13.353\,384$	$C_6 = 1.373\,241\,2$
$D = 1.241\,314$	$C_8 = 0.425\,378\,5$
$r_m = 2.967\,3$ Å	$C_{10} = 0.178\,100$.

Unless otherwise stated the curves shown in this article have been evaluated using the Lennard-Jones potential.

1.2 PARTIAL WAVE ANALYSIS OF THE COLLISION. — For the three systems the phase shifts δ_l have been calculated by numerical integration of the radial wave equation according to a standard procedure [10, 18]. The numerical results are reported in figures 1, 2, 3, as functions of a dimensionless parameter k^* which is the product of the wave number k by the « diameter » of the atoms σ (defined by $V(\sigma) = 0$). As can be seen on the figures the low energy behaviour of the three systems is quite different.

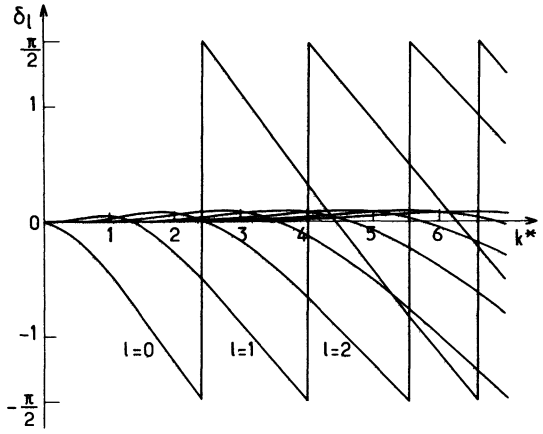

Fig. 1. — Collisional phase shift for H↑ as a function of the reduced wave number $k^* = k\sigma$ (σ = 3.687 Å is the diameter of the interaction potential). For $k^* = 1$ the kinetic energy of the relative motion is 3.54 K. The scattering length is small (0.72 Å) and positive; the repulsive interaction is slightly dominant.

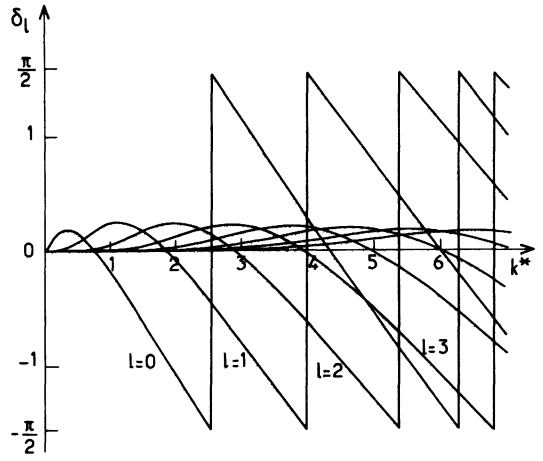

Fig. 2. — Collisional phase shifts for D↑ as a function of the reduced wave number $k^* = k\sigma$ (σ = 3.687 Å). $k^* = 1$ corresponds to a relative kinetic energy of 1.77 K. The scattering length is equal to 3.52 Å and negative; the attractive interaction becomes slightly dominant.

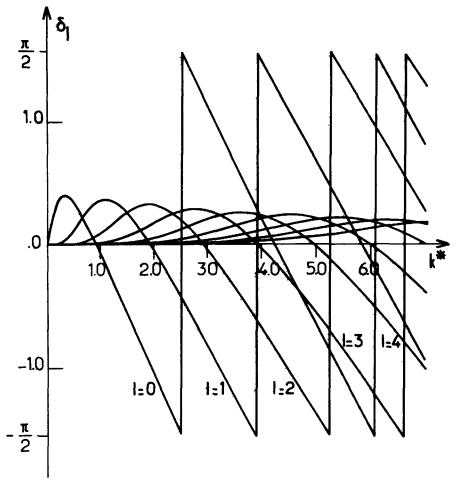

Fig. 3. — Collisional phase shifts for ^{3}He as a function of the reduced wave number $k^* = k\sigma$ (σ = 2.556 Å is the diameter of the Lennard-Jones potential). $k^* = 1$ corresponds to a kinetic energy of 2.46 K. The scattering length is equal to 6 Å and negative; the attractive interaction dominates the low-energy behaviour of the collision but is still insufficient to stabilize a bound state.

Let us first examine the s-wave scattering. In H↑ the low energy $l = 0$ phase shift is negative, which is the signature of a repulsive effective interaction. Nevertheless the balance between attractive and repulsive effects is almost perfect, and the phase shift is very small. This can be measured by the scattering length a_0 defined as usual as :

$$a_0 = - \lim_{k \to 0} \frac{\delta_0(k)}{k}. \qquad (4)$$

For H↑ the scattering length is positive and equal to 0.72 Å. In D↑, due to the larger mass, attractive effects prevail at low energy and the scattering length becomes negative ($a_0 = -3.52$ Å). In ^{3}He the balance between repulsive and attractive effects is still more favourable to the attractive effects and the scattering length is larger, of the order of 6 Å, and negative ([2]).

Another important feature of this analysis is the relative weight of $l \neq 0$ partial waves scattering for a given wave number k^*. At very low wave numbers the scattering is always isotropic, but in D↑ and ^{3}He it becomes very rapidly anisotropic with increasing wave number. In these two systems as soon as $k^* = 1$ (i.e. for energies between 1 and 2 K) the scattering appears to be dominated by the $l \neq 0$ collision channels and the isotropic, low-energy behaviour

([2]) The low energy characteristics of the collision are very sensitive to the interaction potential : for example for ^{3}He the scattering length varies from $a_0 = -6.06$ Å for the Lennard-Jones potential, to $a_0 = -6.97$ Å for the Aziz potential. (On account of the agreement between the Aziz potential and *ab initio* Hartree-Fock calculations in the range 4-5 a.u. this second value is probably the better one.)

cannot be reached unless very low temperatures are achieved. As a consequence the validity of the description of the transport properties in these systems in terms of s-wave pseudo-potentials is limited to the very low temperature range ($T < 100$ mK or less) and a full numerical analysis of the collision is necessary in order to obtain realistic results.

On the other hand, at the highest energies studied in this work the behaviour of the phase shifts is essentially controlled by the repulsive part of the potential. For a repulsive, hard-core potential of radius R_c, the high energy phase shifts behave as :

$$\delta_l(k) \sim \left(- kR_c + \frac{\pi}{2} l \right). \quad (5)$$

The comparison with the exact results shown in figures 1-3 allows the determination of an effective, hard-core radius of the order of σ. As a first consequence, and in contradiction with the low energy case, the high-energy behaviour of the three systems can be described relatively well with σ as a scaling parameter.

1.3 DIFFERENTIAL CROSS SECTIONS. — Combining these phase shifts one obtains the differential cross sections introduced in the collision term of the quantum Boltzmann equation (equation (32) of LL1) : the direct (or classical) cross section is as usual :

$$\sigma_k = \frac{1}{k^2} \sum_{l,l'} e^{i(\delta_l - \delta_{l'})} (2l + 1)(2l' + 1) \sin \delta_l \times \times \sin \delta_{l'} P_l(\cos \theta) P_{l'}(\cos \theta) \quad (6)$$

and the two « exchange cross sections » are given by :

$$\sigma_k^{ex} = \frac{1}{k^2} \sum_{l,l'} (-1)^l (2l + 1)(2l' + 1) \cos(\delta_l - \delta_{l'}) \times \times \sin \delta_l \sin \delta_{l'} P_l(\cos \theta) P_{l'}(\cos \theta) \quad (7)$$

$$\tau_k^{ex} = \frac{1}{k^2} \sum_{l,l'} (-1)^l (2l + 1)(2l' + 1) \sin(\delta_{l'} - \delta_l) \times \times \sin \delta_l \sin \delta_{l'} P_l(\cos \theta) P_{l'}(\cos \theta). \quad (8)$$

We show in figures 4 and 5 some of these results for H↑ and ^{3}He systems (the D↑ patterns, being quite similar to the ^{3}He ones, have been omitted).

The first remarks deal with the similarities between the different systems. As a function of $k^* = k\sigma$, and for $2 < k^* < 7$, the general features of the angular patterns appear to be similar in each system : in particular the number of lobes of the angular diagrams depends almost exclusively on the k^* value. In this range of wave numbers the main effect appears to be that of diffraction by the repulsive potential of diameter σ. All the cross sections reflect the quantum oscillations due to this diffraction effect. At the highest wave numbers studied here the σ_k cross section is strongly peaked in the forward direction at an angle of order $2\pi/k\sigma = 2\pi/k^*$; the σ_k^{ex} cross section, which

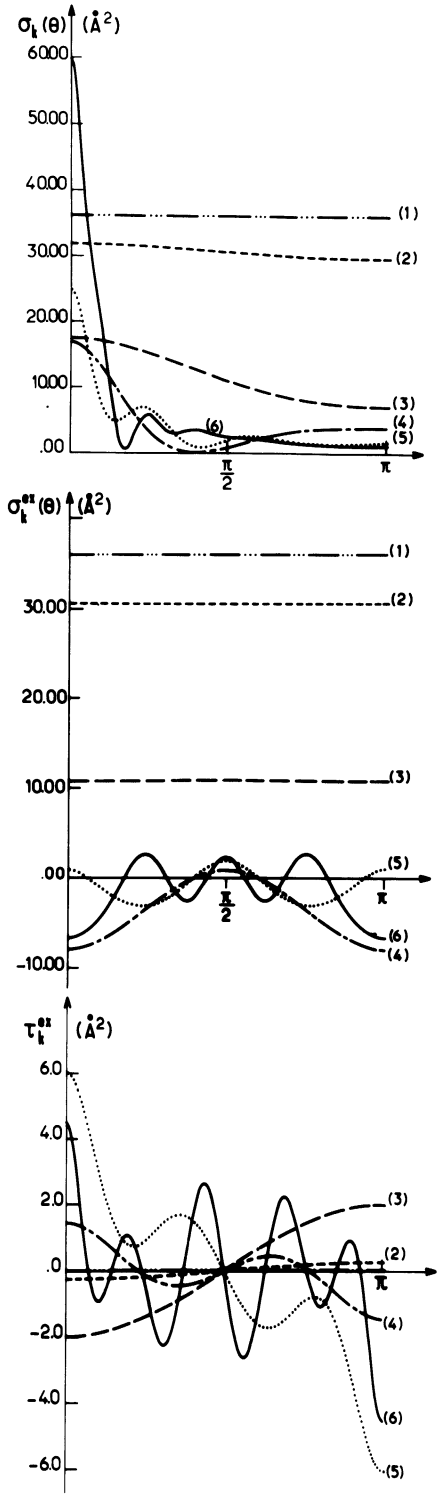

Fig. 4. — Differential cross sections for ^{3}He as a function of the scattering angle. The correspondence between the labels of the curves and the wave vector is the following : (1) $k^* = 1/210$; (2) $k^* = 3/210$; (3) $k^* = 9/210$; (4) $k^* = 1$; (5) $k^* = 3$; (6) $k^* = 7$. One can notice in the figure the isotropic low-energy behaviour of the differential cross sections ($k^* \leqslant 1/70$). At the highest k^* studied here the ordinary scattering cross section appears to be strongly peaked in the forward direction. The exchange cross sections do not decrease very quickly with increasing energy, but oscillate more and more rapidly, reflecting the domination of partial waves with increasing l values.

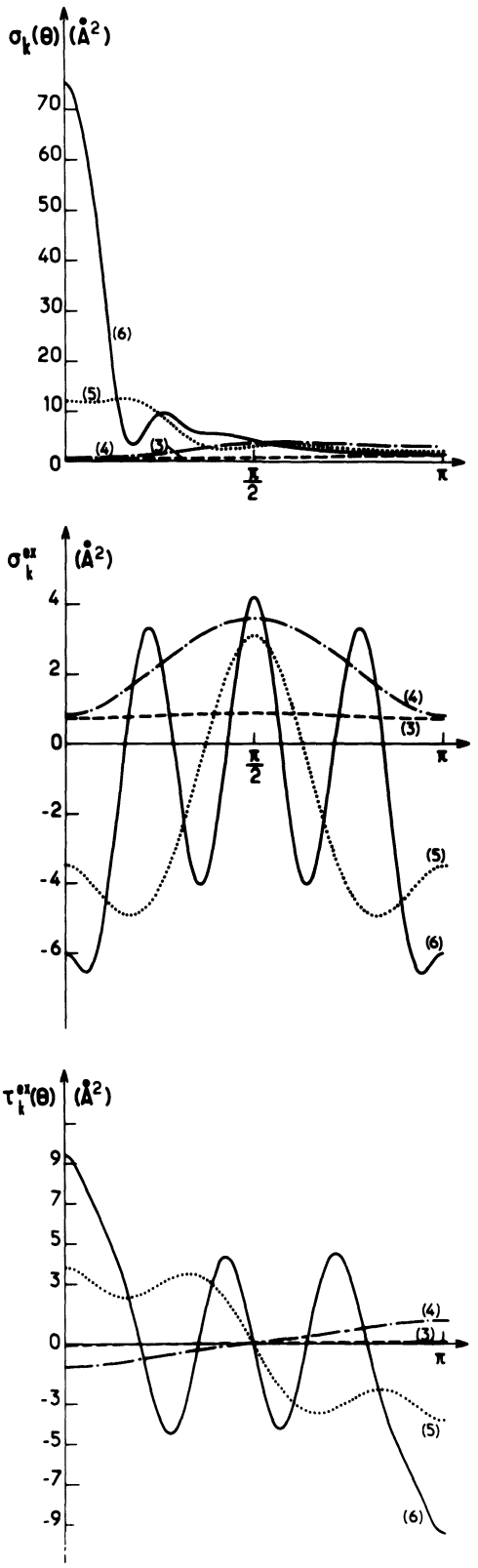

Fig. 5. — Differential cross sections for H↑ as a function of the scattering angle. Same values of the reduced wave number k^* as in figure 4.

has a forward-backward symmetry, is much weaker and consequently particle scattering occurs essentially in the forward direction. In fact transport phenomena are not sensitive to all the details of the differential cross sections but only to a few angle-averaged ones which we shall now study.

1.4 ANGLE-AVERAGED CROSS SECTIONS. — As usual the averages are defined by the general formula

$$Q^t_{[\sigma]} = 2\pi \int_0^\pi (1 - \cos^t \theta)\, \sigma(\theta) \sin\theta \, d\theta . \quad (9)$$

The calculations of viscosity, heat conductivity, longitudinal spin diffusion and their couplings involve, in the first approximations developed in LL1 and LL2, the three averages :

$$Q^1_{[\sigma_k]} = \frac{4\pi}{k^2} \sum_{l=0}^{\infty} (l+1) \sin^2(\delta_l - \delta_{l+1}) \quad (10)$$

$$Q^2_{[\sigma_k]} = \frac{4\pi}{k^2} \sum_{l=0}^{\infty} \frac{(l+1)(l+2)}{(2l+3)} \sin^2(\delta_l - \delta_{l+2}) \quad (11)$$

$$Q^2_{[\sigma_{\hat{k}}{}^x]} = \frac{4\pi}{k^2} \sum_{l=0}^{\infty} (-1)^l \frac{(l+1)(l+2)}{(2l+3)} \sin^2(\delta_l - \delta_{l+2}) . \quad (12)$$

The first two averages $Q^1_{[\sigma_k]}$ and $Q^2_{[\sigma_k]}$ of the « distinguishable particle cross section » σ_k have the same qualitative variations as a function of the energy of the encounter. We have chosen to focus our attention on $Q^2_{[\sigma_k]}$ which appears in the expressions of heat conductivity and viscosity combined with the exchange cross section $Q^2_{[\sigma_{\hat{k}}{}^x]}$. The results for H↑ and ^{3}He are shown in figures 6 and 7. As expected, in the s-wave approximation the low energy limit of $Q^2_{[\sigma_k]}$ and $Q^2_{[\sigma_{\hat{k}}{}^x]}$ is the same and equals $\frac{8\pi}{3} a_0^2$. However, as the energy increases the contribution of the p, d, ... waves becomes important and the two cross sections behave differently; due to the alternate contributions of even and odd phase shifts $Q^2_{[\sigma_{\hat{k}}{}^x]}$ exhibits a few oscillations and rapidly vanishes.

If we now compare the two systems H↑ and ^{3}He we see some marked differences in the low-energy behaviour. In H↑, due to the balance between attraction and repulsion discussed in section 1.2, the $Q^2_{[\sigma_k]}$ and $Q^2_{[\sigma_{\hat{k}}{}^x]}$ cross sections are very weak at zero energy and then go through a maximum near $k^* = 1.5$ (i.e. for an energy of the relative motion of the order of 8 K); in ^{3}He, on the contrary, due to the low-energy attractive effect, $Q^2_{[\sigma_k]}$ and $Q^2_{[\sigma_{\hat{k}}{}^x]}$ take their largest value at $k^* = 0$ and then rapidly decrease as functions of k.

Let us now turn to the « identical spin rotation » effects which govern the oscillatory transverse spin diffusion. They are described by two exchange cross sections

$$Q^1_{[\tau^{ex}]} = \frac{8\pi}{k^2} \sum_{l=0}^{\infty} (-1)^l (l+1) \sin(\delta_l - \delta_{l+1}) \times \times \sin\delta_l \sin\delta_{l+1} \quad (13)$$

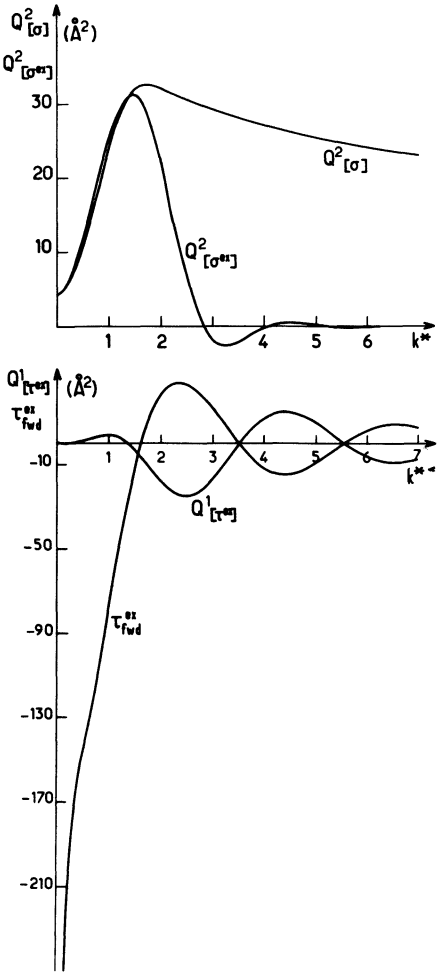

Fig. 6. — Angle-averaged monochromatic cross sections for H↑. $Q^2_{[\sigma]}$ and $Q^2_{[\sigma^{ex}]}$ are the two cross sections involved in the calculation of the heat conduction coefficient. The very low zero energy value is a characteristic feature of H↑ due to the quasi Ramsauer effect already discussed in section 1.2. As expected in the s-wave approximation, the behaviour of $Q^2_{[\sigma]}$ and $Q^2_{[\sigma^{ex}]}$ is identical for $k^* < 1$, but the exchange cross section decreases very rapidly in the semi-classical region ($k^* > 3$). The two cross sections $Q^1_{[\tau^{ex}]}$ and τ^{ex}_{fwd} measure the « identical spin rotation » effect in the scattered and transmitted beam. As expected, the low-energy behaviour is totally dominated by the effect in the transmitted beam. For $k^* > 1$ each contribution decreases slowly with increasing energy but the sum of the two contributions vanishes as quickly as $Q^2_{[\sigma^{ex}]}$. As explained in section 1.3 it is a feature of the semi-classical region where the quantum interference effects still exist but are rubbed out by angular averaging.

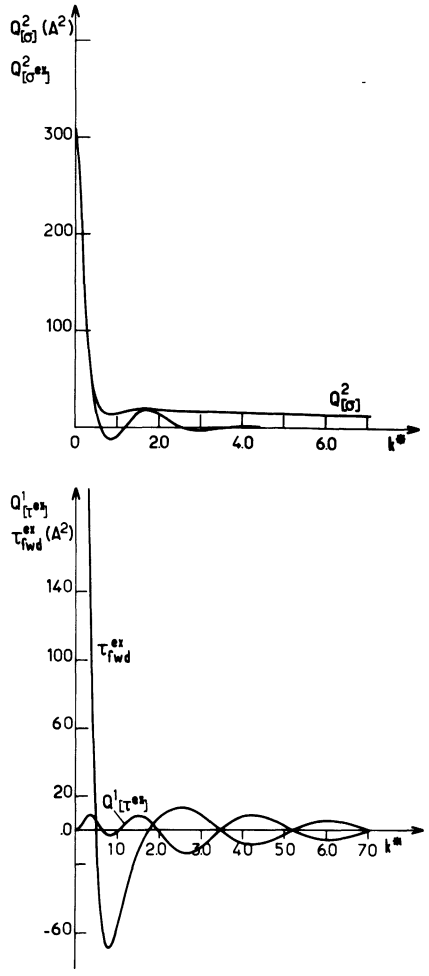

Fig. 7. — Angle-averaged monochromatic cross sections for ^{3}He. Same comments as in figure 6.

which measures the identical spin rotation in the scattered wave and

$$\tau^{ex}_{fwd} = \frac{2\pi}{k^2} \sum_{l=0}^{\infty} (-1)^l (2l+1) \sin 2\delta_l \qquad (14)$$

which measures the identical spin rotation effect in the transmitted beam and is not reducible to an angular average of the quantity $\tau^{ex}_k(\theta)$ ([3]). From that point of view, the previously-studied averaged cross sections (10)-(12) collect both the effects of the collision in the transmitted wave and in the spherically scattered wave and are comparable to the sum

$$Q^1_{[\tau^{ex}]} + \tau^{ex}_{fwd} = \frac{2\pi}{k^2} \sum (-1)^l (2l+1) \times \times \sin 2(\delta_l - \delta_{l+1}). \qquad (15)$$

As expected in LL2, the low-energy behaviours of $Q^1_{[\tau^{ex}]}$ and τ^{ex}_{fwd} are quite different; in the low-energy limit $Q^1_{[\tau^{ex}]}$ tends towards zero while τ^{ex}_{fwd} diverges as $1/k$. At low energy the dominant feature of the collision is actually this rotation of the spins in the transmitted beam. Moreover, this effect decreases very slowly with the energy of the impinging particles and is still important at the highest wave numbers studied here.

([3]) As explained in LL1 there is no conservation rule on individual spin which relates $\tau^{ex}_k(\theta)$ and τ^{ex}_{fwd} as is the case for example for σ_{TOT} and $\sigma_k(\theta)$ or σ^{ex}_{fwd} and $\sigma^{ex}_k(\theta)$ through the conservation of the particles.

However, it clearly appears in figures 6 and 7 that the effect in the transmitted wave is almost exactly balanced by the average effect in the scattered wave, so that the sum $Q^1_{[\tau^{ex}]} + \tau^{ex}_{fwd}$ (like $Q^2_{[\sigma^{ex}]}$) rapidly goes to zero with increasing k and becomes quite negligible when k^* is larger than 3 or 4. Such an effect is typical of semi-classical collisions [19]. When the wavelength of the particles becomes smaller than the range of the interaction potential ($k^* > 1$) more and more phase shifts are necessary to describe the collision and the dominant l values are of the order of magnitude $l \sim k^*$. (This can easily be checked on the angular diagrams of figures 4 and 5 where the number of lobes is a signature of the dominant partial waves.) If we consider a superposition of spherical waves with large angular momentum l ($l_0 + \Delta l < l < l_0 + \Delta l$, $l_0 \gg 1$, $\Delta l < l_0$) they form a laterally-localized wave packet that can be characterized by a classical impact parameter $b = k^{-1} l_0$. This wave packet will be predominantly scattered in an angle θ directly connected to the l_0 value. (In the WKB approximation $\theta = \pm 2\left(\frac{d\delta_l}{dl}\right)_{l=l_0} + 2\pi n.$) Most of the quantum paths, and especially the most important in the scattering ($l_0 \sim k^*$), can then be described by classical trajectories, which should preclude the observation of exchange effects : in fact it clearly appears in this example that the interference effects do subsist in the semi-classical region (Figs. 4 and 5) but the angular selectivity of the transport process becomes insufficient for their observation and they are washed out by the angular averaging which leads to formula (12) and (15).

2. **Transport phenomena in H↑, D↑, ^{3}He.** — From the knowledge of the collision it is straightforward to evaluate the transport coefficient in partially-polarized quantum systems. The theory described in LL1 and LL2 will be only briefly summarized here. The treatment is based on the standard Chapman-Enskog solution of the Boltzmann quantum equation, which supposes the density to be low and the gradients of the physical quantities to be small. In the first approximation (Navier-Stokes approximation) the flux of the molecular properties appears to be proportional to the first-order derivatives of the physical macroscopic quantities (temperature, magnetization...). In this approximation, which is the framework of all the results given here, the numerical solution of the problem can only be approached by some approximate method. (As usual we have used an expansion of the density operator using a basis of Sonine polynomials, and have used one or two terms of this expansion; it is to this last expansion that we shall refer later on in the discussion.) The transport coefficients appear then as homographic functions of collision integrals which are various averages of the quantum cross sections (10)-(15) over the Boltzmann distribution. The definition of the Ω collision integrals is, as usual :

$$\Omega^{(t,s)}_{[\sigma]} = \frac{1}{(\pi m\beta)^{1/2}} \int_0^\infty d\gamma\, e^{-\gamma^2}\, \gamma^{2s+3}\, Q^t_{[\sigma]} \qquad (16)$$

where $Q^t_{[\sigma]}$ is the angular averaged cross section evaluated for the wavenumber $k = (m/\beta)^{1/2}\, \gamma/\hbar$, m being the mass of the particles, and $\beta = 1/kT$.

The phenomena discussed in this paper involve collision integrals Ω of the three differential cross sections $\sigma_k(\theta)$, $\sigma^{ex}_k(\theta)$ and $\tau^{ex}_k(\theta)$, and similar averages on τ^{ex}_{fwd} defined in LL2 (Eq. 4) as :

$$\Xi^{(s)}_{[\tau^{ex}_{fwd}]} = \frac{1}{\sqrt{\pi m\beta}} \int_0^\infty d\gamma\, e^{-\gamma^2}\, \gamma^{2s+3}\, \tau^{ex}_{fwd} \qquad (17)$$

where τ^{ex}_{fwd} is the cross section (14) evaluated for the wavenumber $k = (m/\beta)^{1/2}\, \gamma/\hbar$.

These integrals have been computed by means of Simpson's rule together with the Newton 3/8 rule for temperatures ranging from 40 mK to 10 K and are believed to be accurate to within 1 part in 100 in the most unfavourable cases ($\Xi^{(s)}_{[\tau^{ex}_{fwd}]}$ and $\Omega^{(1,s)}_{[\tau^{ex}]}$ for $T \gtrsim 1$ K) and in general to the order of a few parts in 1 000. Some of these integrals have already been computed by Monchick *et al.* [12], their results agree with ours within the quoted uncertainties ([4]). With the help of these integrals and of the formulas given in LL1 and LL2 we are now able to evaluate the viscosity and heat conduction, as well as spin diffusion coefficients ([5]).

2.1 HEAT CONDUCTIVITY. — The heat conductivity of H↑, D↑ and ^{3}He, and its variations with the nuclear polarization M, are reported in figures 8, 9 and 10. (In the D↑ case, the nuclear spin of which is equal to one, we have for simplicity considered only the two situations where the nuclear polarization is either zero or complete.) For the spin 1/2 case this coefficient is in the first approximation equal to

$$K(M) = K(0)\, \frac{1 - \xi_1 M^2}{1 - \xi_2 M^2} \qquad (18)$$

where $K(0)$ is the coefficient of the unpolarized gas (equation (61) of LL1) and the ξ_1 and ξ_2 coefficients

([4]) In fact the inaccuracies due to an insufficient knowledge of the potentials are much larger than the numerical uncertainties and can probably range from a few % to ten or fifteen percent in the most unfavourable cases. Moreover, the very low temperatures results ($T < 50$ mK for H↑ and $T < 250$ mK for ^{3}He) are presumably unrealistic due to the neglect of the hyperfine interaction.

([5]) Tables of collisions integrals for the three systems H↑, D↑ and ^{3}He, described by the afore-mentioned potentials, are available on request.

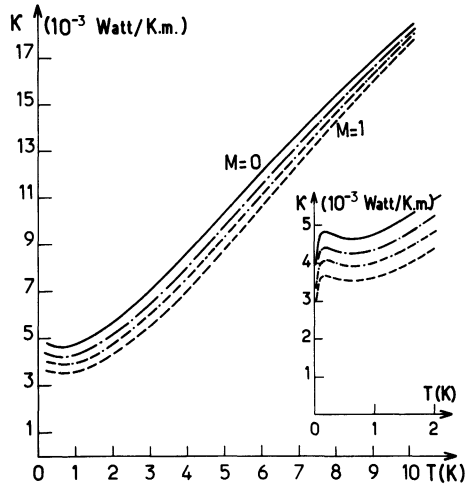

Fig. 8. — Heat conductivity *versus* temperature T and nuclear polarization M in H↑. The heat conductivity monotonically decreases with increasing polarization.

— full line curve $M = 0$;
—·—·— $M = 0.6$;
--·--·-- $M = 0.8$;
------ full polarization $M = 1$.

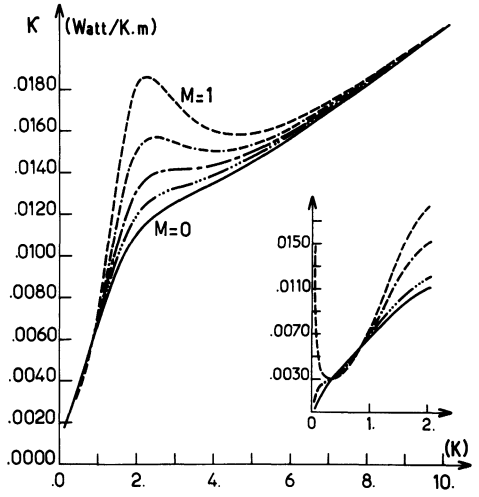

Fig. 10. — Heat conductivity in ^{3}He *versus* temperature and nuclear polarization M :

— $M = 0$;
—·····— $M = 0.4$;
—·— $M = 0.6$;
·--·-- $M = 0.8$;
--- $M = 1$.

Same comments as in figure 9.

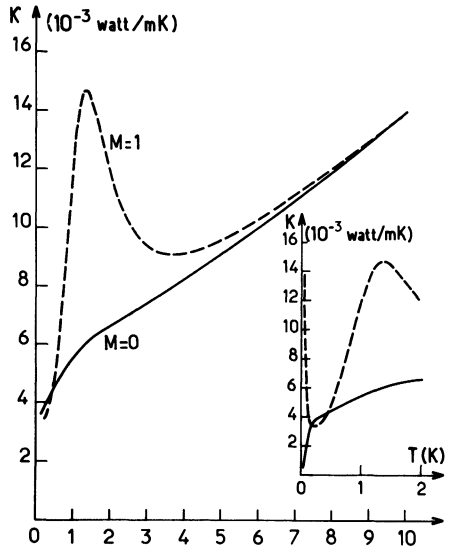

Fig. 9. — Heat conductivity in D↑ *versus* temperature, for zero nuclear polarization (full line) and full nuclear polarization (dashed line). The low-temperature divergence of heat conductivity for fully polarized systems is a characteristic feature of fermionic systems; the « bump » at 2 K is a dynamical feature explained in section 2.1.

are expressed as functions of the collision integrals through formulas (56) and (61) of LL1. The curves shown here represent the first approximation described by formula (18) and equation (61) of LL1. Calculation of higher approximations is easily done with the help of the tables of collisions integrals and of equation (24) of LL2. The second-order corrections in the M^2 expansion (equation (24) of LL2) are quite negligible (of the order of 10^{-3}). They are not to be confused with the second-order correction for $K(0)$ which has been studied in reference [12] and amounts typically to a few percent in the observed temperature range (6 % at 3 K).

In the three studied systems the heat conductivity appears to be strongly dependent on the nuclear polarization in a wide range of temperatures; for the lightest case (H↑) the effects are still measurable up to 20 K. On the other hand, these results display a large qualitative difference between boson and fermion systems. In H↑ the heat conductivity varies monotonically with the nuclear polarization and quite smoothly with the temperature. In D↑ and ^{3}He, on the contrary, the variation of heat conductivity with nuclear polarization exhibits a peak at intermediate temperatures and a divergence at very low temperatures ($T < 100$ mK). The low-temperature increase of the conductivity of totally polarized ^{3}He and D↑ is a simple effect of the Fermi statistics : the Pauli principle forbids all scattering in even-l waves, and on the other hand, at low temperature the centrifugal barrier prevents the interaction in all $l \neq 0$ channels; as a result the effective interaction goes to zero with the temperature and the heat conduction (as the viscosity) diverges in fully-polarized fermion systems. It must nevertheless be stressed that this effect appears in a very low-temperature range where the vapour pressure of ^{3}He (and D↑) is probably very low. Moreover, the condition of full polarization is essential; if there are traces of the opposite polarization the low-temperature conductivity will go to zero dominated by the non-vanishing interaction between atoms in

opposite nuclear spin states. From an experimental point of view, the strong change of heat conductivity with nuclear polarization (around 2 K for ^{3}He, 1 K for D↑) is probably of much greater interest and more readily accessible to measurements. The observed « bump » of the heat conductivity in nuclear polarized D↑ and ^{3}He is due to a local phase shift cancellation in the p($l = 1$) and f($l = 3$) waves. (Easily seen on the phase shift diagrams 2 and 3 at $k^* \sim 1.75$, it can be checked on the monokinetic cross sections of figure 7 where it explains the local equality between $Q^2_{[\sigma]}$ and $Q^2_{[\sigma^{ex}]}$.) Such a cancellation is a pure dynamical consequence of the balance between attractive and repulsive interactions. Its observation is made possible in nuclear polarized systems by elimination, through the Pauli principle, of the even channels of interaction. In the H↑ system the variations of the cross sections are much smoother, being always dominated by repulsive effects, and so are the variations of the heat conductivity with nuclear polarization and temperature.

2.2 LONGITUDINAL SPIN DIFFUSION. — As it has been shown in LL2, the spin diffusion in a partially polarized system is not isotropic, the diffusion of the longitudinal component of the polarization being quite different to that of the transverse one. [We call longitudinal (respectively transverse) the component of the polarization parallel (respectively perpendicular) to the main local magnetization.] The oscillatory mode of diffusion of the transverse polarization will be considered later : as a first stage we will focus our interest on the purely damping mode of longitudinal spin-diffusion. This process has an exact analogue in concentration diffusion in classical mixtures : the diffusion of the « up » specie in the « down » one is controlled in the first approximation by the collision between distinguishable atoms (cross section σ_k) and the diffusion of the longitudinal component of the polarization is then independent of M (the analogue of the chemical concentration) and is given by the formula

$$\mathbf{J}(M_Z) = - D_0 \nabla M_Z$$

with :

$$D_0 = \frac{3}{8} \frac{1}{nm\beta} \frac{1}{\Omega^{(1,1)}_{[\sigma]}}. \qquad (19)$$

The general features of the first approximation can be seen in figures 15 and 16 (full line curves) for H↑ and ^{3}He. A more refined approximation (section 2 of LL2) predicts a weak dependence of this coefficient on the nuclear polarization, which is easily evaluated with the help of formulas (22) and (23) of LL2. The total correction due to the second approximation is rather small and does not exceed 5 %, the M dependence of the process being still smaller and at the most of the order of 2 % (in the H↑ case for $T < 200$ mK). The longitudinal spin diffusion mode thus appears to be fairly insensitive to exchange effects but the symmetry principle is at the origin of a new effect : the mode coupling between heat conduction and longitudinal spin diffusion.

2.3 MODE COUPLING BETWEEN SPIN DIFFUSION AND LONGITUDINAL HEAT DIFFUSION. — In the presence of both a temperature and a longitudinal magnetization gradient the fluxes of heat and spin polarization **M** appear to be coupled by the symmetry effects. The flux of heat reads :

$$\frac{1}{T}\mathbf{J}_w = - \{ K(M) \nabla \operatorname{Log} T + \varepsilon L_{12}(M) \nabla M_Z \} \qquad (20)$$

the flux of the longitudinal component of the polarization being then given by :

$$\mathbf{J}_{M_Z} = - \{ D(M) \nabla M_Z + \varepsilon L_{21}(M) \nabla \log T \} \qquad (21)$$

with $\varepsilon = \pm 1$ for bosons (respectively fermions).

The algebraic formulas for these two cross coefficients $L_{12}(M)$ and $L_{21}(M)$ are given in LL2 (equations (22) and (25)); the numerical ratio of the cross coefficients to the main ones are shown in figures 11

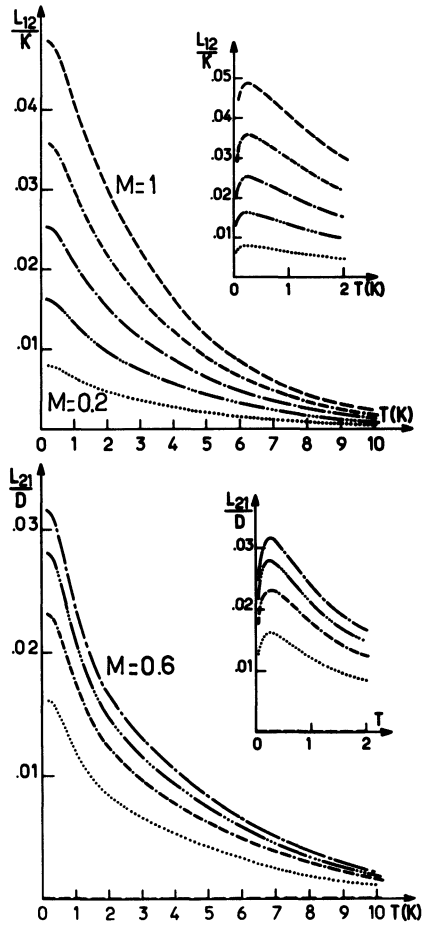

Fig. 11. — Coupling coefficients for the two coupled modes, heat conduction and longitudinal spin diffusion in H↑, *versus* temperature and nuclear polarization M, M varying from 0 to 1 with :

—— $M = 0$; —·—· $M = 0.6$;
· · · · · · $M = 0.2$; —·——·— $M = 0.8$;
—· · ·— $M = 0.4$; ——— $M = 1$.

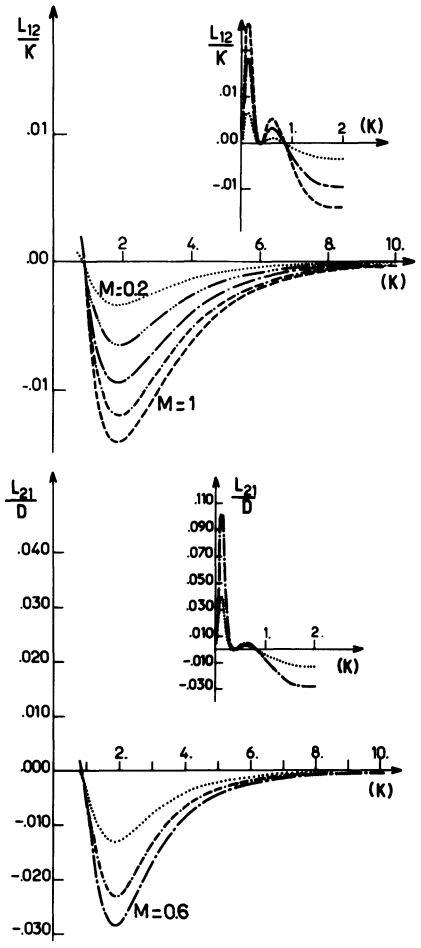

Fig. 12. — Cross coefficients for the two coupled modes (heat conduction and longitudinal spin diffusion) in ^{3}He. (Same legend as in figure 11.)

and 12 for H↑ and ^{3}He. The analogies between the two cross coefficients of the same gas are merely an exhibition of the Onsager relation as explained in appendix III of LL2. Nevertheless, the Onsager relation between the two cross coefficients depends on the nuclear polarization M, so that the M dependence of the two terms L_{12} and L_{21} is different. The coupling of the heat flux with a magnetization gradient is a monotonically increasing function of the polarization, whereas the coupling of the spin flux with a temperature gradient increases with increasing polarization, has a maximum for a nuclear polarization of about 60 % and then decreases towards zero as the polarization becomes complete. One could envisage using these couplings in order to stabilize or possibly over-polarize a small region of a sample by a gradient of temperature, but the order of magnitude and the M dependence of the L_{21} coefficient are unhappily not very favourable to that prospect.

The numerical results call for a last remark : even at the lowest temperatures here considered (40 mK), and especially in ^{3}He, the results still differ significantly from those obtained in LL2 in the scattering-length approximation. The collision integrals involved in the computation of these coefficients favour the high energy part of the Boltzmann distribution function, as a consequence they are still sensitive to p and d scattering at a temperature as low as 40 mK, and the scattering-length approximation will never be a good approximation in these gases.

2.4 TRANSVERSE SPIN DIFFUSION AND SPIN WAVES. — As explained in section 2.2 the direction Oz of the local magnetization is an anisotropy axis for the spin diffusion, and parallel and perpendicular polarizations evolve quite differently. The general form of the transverse polarization current is :

$$\mathbf{J}(M_x) = - D_\perp[\nabla \mathbf{M}_x + \varepsilon M \mu_\perp \nabla \mathbf{M}_y] \quad (22)$$

$$\mathbf{J}(M_y) = - D_\perp[- \varepsilon M \mu_\perp \nabla \mathbf{M}_x + \nabla \mathbf{M}_y]. \quad (23)$$

In the first approximation the transverse spin diffusion coefficient $D_\perp$ is just given by :

$$D_\perp = \frac{D_0}{1 + \mu^2 M^2} \quad (24)$$

where D_0 is the « classical » diffusion coefficient given by equation (19) and μ has the following expression

$$\mu = \frac{\Omega^{(1,1)}_{[\tau^{ex}]} + \Xi^{(1)}_{[\tau \tilde{F} \tilde{\alpha} d]}}{\Omega^{(1,1)}_{[\sigma]}}. \quad (25)$$

In addition to the usual damping terms, equations (22) and (23) exhibit an oscillatory behaviour due to the « identical spin rotation » discussed in LL1 and LL2. The ratio of the angular precession frequency of these spin waves to the damping constant is directly measured by the constant $\varepsilon M \mu_\perp$, which reduces in the first approximation to $\varepsilon M \mu$ (6). The coefficients μ and $D_\perp$ evaluated in this first approximation are reported in figures 13 to 14.

As predicted in LL2, the μ coefficients take very large values at low temperatures. (They are predicted to diverge as $T^{-1/2}$ when T goes to zero.) Moreover, as can be seen in figures 13 and 14, they are still important in a large range of temperature.

To illustrate the uncertainty due to the potential, we have shown in figure 14 the μ coefficient of ^{3}He calculated with the two afore-mentioned potentials described in section 1.1.

As can be seen in this example, the uncertainty due to the potential never exceeds 10 %; it takes the largest value in the intermediate temperature range where the competition between attractive and repulsive effects is maximum. Experiments in the temperature range 1-2 K would then be a very stringent test of the potential.

Associated with this transverse precession of the spins is a slowing down of the diffusion exhibited in figures 15 and 16. In these figures we can evaluate

(6) The second approximation for $D_\perp$ and $\mu_\perp$ are given in LL2, formulas (26), (27) and appendix II.

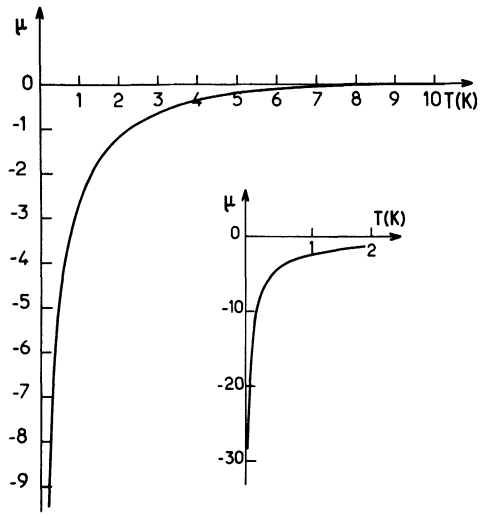

Fig. 13. — « Identical spin rotation » coefficient μ in H↑ *versus* temperature.

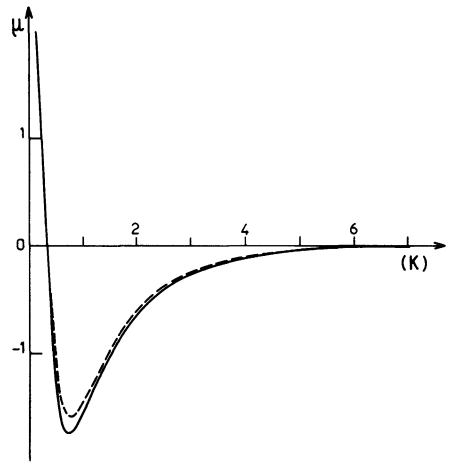

Fig. 14. — « Identical spin rotation » coefficient μ in ^{3}He *versus* temperature. The full line curve has been calculated with the Lennard-Jones potential (Eq. 2), the dashed one with the Aziz potential (Eq. 3).

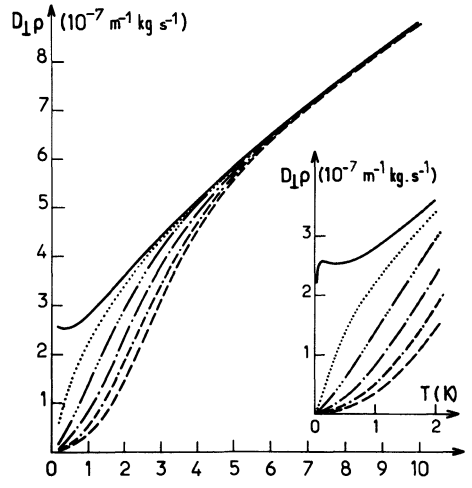

Fig. 15. — Transverse spin diffusion coefficient in H↑ (same legend as in figure 11 for nuclear polarization). The full line curve (zero polarization) is a good first approximation to the longitudinal spin diffusion coefficient for any value of the polarization.

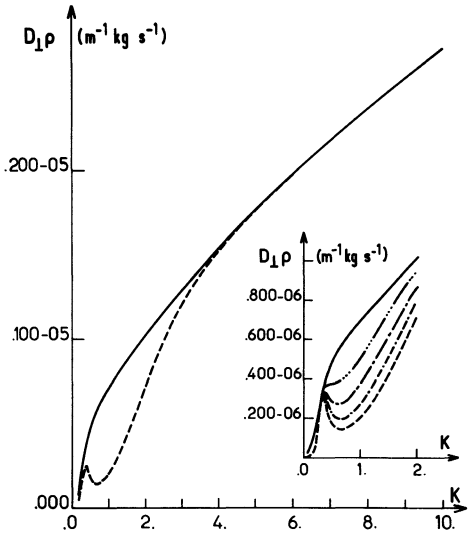

Fig. 16. — Transverse spin diffusion coefficient in ^{3}He. (Same legend as in figure 10 for nuclear polarization.) The full line curve is a good first approximation to the longitudinal spin diffusion coefficient for any value of the polarization.

both the blocking of the transverse spin current and the anisotropy of the spin diffusion. (The zero polarization curves for $D_\perp$ are just equal to D_0 which is a very good first approximation to the M_Z diffusion coefficient.) They appear to be quite important in the two studied systems.

Similar macroscopic effects have been predicted [7] and measured [8] in dense Fermi liquids at very low temperatures (in the collisionless regime at $T < 20$ mK). The present study shows that such effects are not limited to degenerate fermionic systems but also occur in both fermionic and bosonic gases in a very large range of temperature. Spin echo measurements, or spin relaxation in inhomogeneous magnetic field [20], are likely to be most sensitive to these effects and to give a direct measurement of the « identical spin rotation » effect.

Acknowledgments. — The author is very grateful to B. Shizgal who gave her program for phase shift calculations with many helpful comments, and thanks F. Laloë for many useful discussions.

References

[1] LHUILLIER, C., LALOË, F., *J. Physique* **43** (1982) 197.
[2] LHUILLIER, C., LALOË, F., *J. Physique* **43** (1982) 225.
[3] BENNAKKER, J. J. M., *Lecture Notes in Physics* **31** (1974) 413, eds. Kirczenow G. and Marro J. (Springer-Verlag).
[4] KAGAN, Y., MAXIMOV, L. A., *Sov. Phys. JETP* **32** (1971) 1116.
[5] BASHKIN, E. P., MEYEROVICH, A. E., *Sov. Phys. Usp.* **23** (1980) 156.
[6] GREYWALL, D. S., PAALANEN, M. A., *Phys. Rev. Lett.* **46** (1981) 1292.
[7] LEGGETT, A. J., *J. Phys. C* **12** (1970) 447.
[8] CORRUCINI, L. R., OSHEROFF, D. D., LEE, D. M., RICHARDSON, R. C., *Phys. Rev. Lett.* **27** (1971) 650 ; *J. Low. Temp. Phys.* **8** (1972) 229.
[9] CLINE, R. W., GREYTAK, T. J., KLEPPNER, D., *Phys. Rev. Lett.* **47** (1981) 1195 ;
SPRIK, R., WALRAVEN, J. T. M., VAN YPEREN, G. H., SILVERA, I. F., *Phys. Rev. Lett.* **49** (1982) 153.
[10] BERNSTEIN, R. B., *Adv. Chem. Phys.* **10** (1964) 75.
[11] MUNN, R. J., SMITH, F. J., MASON, E. A., MONCHIK, L., *J. Chem. Phys.* **42** (1965) 537.
[12] MONCHIK, L., MASON, E. A., MUNN, R. J., SMITH, F. J., *Phys. Rev.* **139** (1965) A.1076.
[13] FREED, J. H., *J. Chem. Phys.* **72** (1980) 1414.
[14] LEFEVRE, V., NACHER, P. J., LHUILLIER, C. and LALOË, F., to be published in *J. Physique*.
[15] KOLOS, N., WOLNIEWICZ, L., *Chem. Phys. Lett.* **24** (1974) 457.
[16] SILVERA, I. F., *Rev. Mod. Phys.* **52** (1980) 393.
[17] AZIZ, R. A., NAIN, V. P. S., CARLEY, J. S., TAYLOR, W. L. and MC CONVILLE, G. T., *J. Chem. Phys.* **70** (1979) 4330.
[18] SHIZGAL, B., private communication.
[19] See for instance : NEWTON, R. G., in *Scattering theory of waves and particules* (Mc Graw Hill) 1966, XVIII.
[20] LEFEVRE, V., NACHER, P. J., LALOË, F., *J. Physique* **43** (1982).